How to cite: *Angew. Chem. Int. Ed.* **2024**, *63*, e202313655
doi.org/10.1002/anie.202313655

Asymmetric Catalysis

Nickel-Catalyzed Asymmetric Propargyl-Aryl Cross-Electrophile Coupling

*Linlin Ding, Yue Zhao, Hongjian Lu, Zhuangzhi Shi, and Minyan Wang**

Abstract: Performing asymmetric cross-coupling reactions between propargylic electrophiles and aryl nucleophiles is a well-established method to build enantioenriched benzylic alkynes. Here, a catalytic enantioselective propargyl-aryl cross-coupling between two electrophiles was achieved for the first time in a stereoconvergent manner. Propargylic chlorides were treated with aryl iodides as well as heteroaryl iodides in the presence of a chiral nickel complex, and manganese metal was used as a stoichiometric reductant, allowing for the construction of a propargyl C-aryl bond under mild conditions. An alternative dual nickel/photoredox catalytic protocol was also developed for this cross-electrophile coupling in the absence of a metal reductant. The potential utility of this conversion is demonstrated in the facile construction of stereoenriched bioactive molecule derivatives and medicinal compounds based on the diversity of acetylenic chemistry. Detailed experimental studies have revealed the key mechanistic features of this transformation.

Introduction

Alkynes which contain propargylic stereogenic centers are important structural motifs in natural products and biologically active compounds, such as molecules **I**–**IV**; alkynes confer valuable structural, conformational and metabolic properties (Figure 1a).[1] In addition, the acetylenic carbon-carbon triple bond is an important synthon in organic synthesis, providing access to a wide variety of downstream transformations.[2] Therefore, considerable effort has been dedicated to developing enantioselective approaches for the synthesis of propargylic stereogenic centers during the last decades.[3] In this context, the catalytic asymmetric propargylic substitution reaction is among the most efficient and prevalent tools for the efficient generation of chiral propargylic compounds (Figure 1b). This strategy involves two approaches to generate the stereogenic center depending upon the nature of the applied propargylic electrophiles. In the case of a propargylic skeleton bearing a terminal alkyne moiety, enantioselective propargylic substitution with different soft nucleophiles can proceed through metal-allenylidene intermediates enabled by ruthenium[4] or copper[5] catalysts. For internal alkynes, the catalytic enantioconvergent cross-coupling of racemic propargylic electrophiles with soft and hard nucleophiles through reductive elimination[6] or allenic substitution[7] has been achieved with Ni and/or Cu catalysts.

Due to the importance of chiral benzylic alkyne skeletons, substantial progress has been made for catalytic asymmetric synthesis, mostly by merging propargylic electrophiles and aryl nucleophiles (Figure 1c). In pioneering work, Fu and co-workers performed nickel-catalyzed asymmetric Negishi coupling between racemic propargylic halides[8] or carbonates[9] with aryl-zinc reagents via a stereoconvergent process to furnish the corresponding propargylic arylation products. Moreover, arylboronate esters could be used as suitable coupling partners in copper-catalyzed enantioselective Suzuki–Miyaura coupling.[10] In 2017, Tortosa reported a copper-catalyzed stereospecific Kumada-type coupling reaction starting from enantioenriched propargylic ammonium salts and aryl-Grignard reagents via an S_N2 pathway.[11] To avoid the necessity of organometallic reagents, the Liu group recently developed an elegant route involving a copper-catalyzed stereoconvergent Sonogashira $C(sp^3)$–C(sp) cross-coupling of terminal alkynes with racemic benzyl halides.[12] Considering that aryl halides are often used as precursors for organometallic reagents, we investigated whether these abundant and structurally diverse feedstocks can be used directly to prepare enantioenriched benzylic alkynes.

Transition metal-catalyzed reductive cross-coupling reactions between two electrophiles have captured extensive attention in organic chemistry.[13] Seminal reports showcased the ability of nickel to mediate the reductive homocoupling of aromatic halides to build biaryl products.[14] In recent years, important progress has been achieved for the enantioselective form under reducing conditions.[15] These reactions have proven particularly useful for the asymmetric coupling of benzylic electrophiles with acyl chlorides, aryl, heteroaryl and vinyl halides, which have been explored by Reisman[16] and Doyle[17] successively. Our group also uncovered a nickel-catalyzed defluoroalkylation of *gem*-difluoroalkenes with benzyl chlorides, showing excellent stereoselectivity and enantioselectivity.[18] In sharp contrast, much less attention has been focused on propargylic electrophiles in reductive cross-coupling, and a dominant prefer-

[*] L. Ding, Dr. Y. Zhao, Prof. Dr. H. Lu, Prof. Dr. Z. Shi, Prof. Dr. M. Wang
State Key Laboratory of Coordination Chemistry, Chemistry and Biomedicine Innovation Center (ChemBIC), School of Chemistry and Chemical Engineering, Nanjing University
Nanjing 210023 (China)
E-mail: wangmy@nju.edu.cn

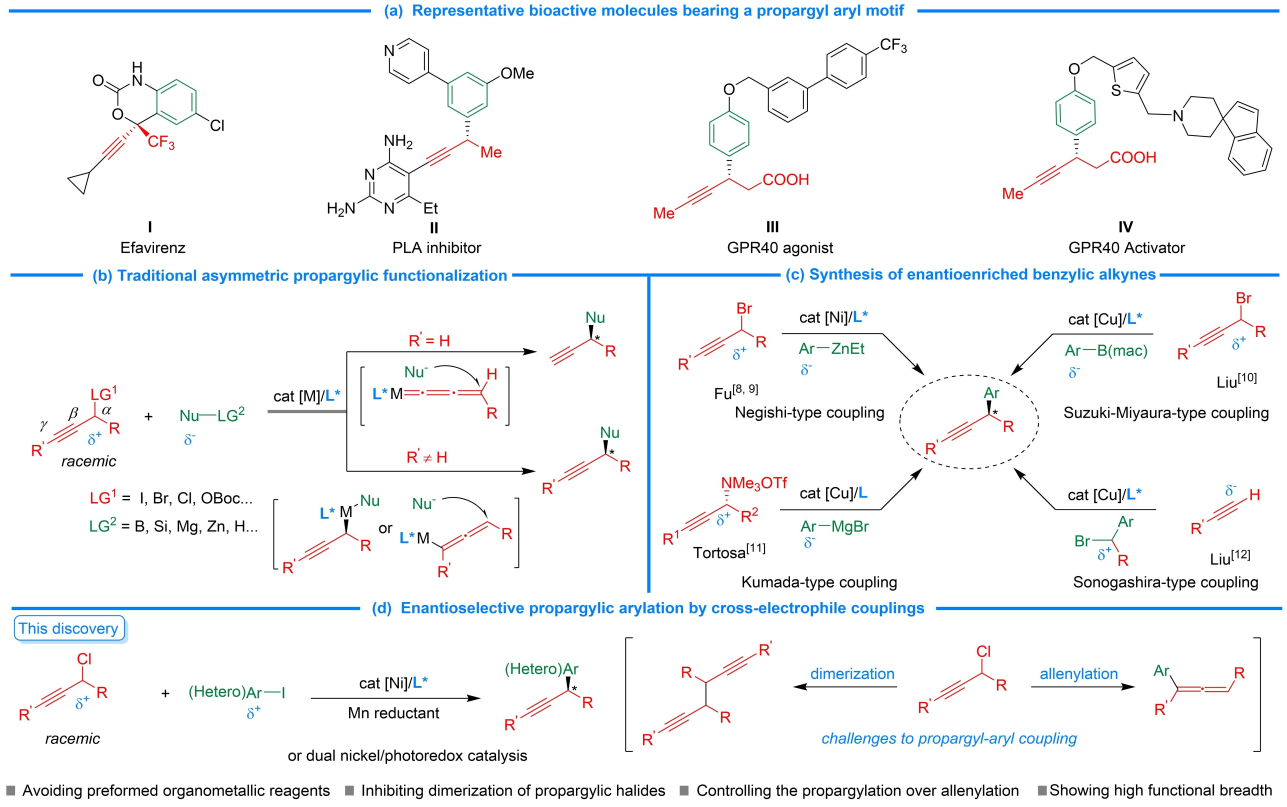

Figure 1. Strategies for propargylic functionalization.

ence for allenylation has been established experimentally.[19] Here, we first report a highly enantioselective catalytic propargyl-aryl cross-electrophile coupling from readily available feedstocks (Figure 1d). Upon exposure to a nickel catalyst with a chiral bisoxazoline (BiOx) ligand, propargylic chlorides can perform *ipso*-selective arylation with aryl and heteroaryl iodides, showing excellent chemo-, regio- and enantioselectivity.

Results and Discussion

Elegant methods relying on the metal-catalyzed addition of organometallic reagents, such as aryl Grignard, tin, zinc, boron and silane reagents, to aldehydes have been widely developed to form alcohols.[20] To demonstrate the compatibility of our strategy, we reacted iodoarene **2a**, which contains a sensitive aldehyde group, with racemic propargylic chloride **1a** using $NiBr_2$·dme (10 mol %) as a catalyst and a stoichiometric amount of manganese powder as the reductant in THF at 0 °C (Table 1). Cross-coupling did not occur in the presence of pyridine-oxazoline ligand (*S*)-**L1**, but a mixture of *rac*- and *meso*-1,5-diyne **4aa** was formed in a large amount (entry 1). We further screened chiral ligands and found that utilizing the BiOx ligand (*R, R*)-**L2** with two ^{t}Bu substituents led to the desired product **3aa** in trace amounts (entry 2). We were pleased to see that diphenyl-BiOx (*R, R*)-**L3** could dramatically improve the reactivity and inhibit the dimerization, generating **3aa** in 76 % yield with a modest enantiomeric ratio (89/11 er, entry 3). Further investigation of different substituents in BiOx ligands under the optimized conditions confirmed that ligands (*R, R*)-**L4** (91/9 er) and (*R, R*)-**L5** (92/8 er) containing two *iso*-butyl and cyclohexyl groups could provide higher enantioselectivities (entries 4–5). Treatment of (*R, R*)-**L6** bearing two flexible 4-heptyl chains[21] as a ligand resulted in excellent reactivity and enantioselectivity (93 % yield, 95.5/4.5 er, entry 6). The tridentate ligand *(R, R)*-**L7** resulted in almost exclusive dimerization, giving compound **4aa** (entry 7). Under the developed reaction conditions, conducting the reaction at room temperature slightly improved the formation of **3aa** but with an erosion of enantioselectivity (93.5/6.5 er, entry 8). When the amount of Mn was reduced to 2.0 equiv, product **3aa** could still be obtained in 89 % yield without compromising enantioselectivity (entry 9). Other reductants, such as zinc, could also maintain good enantioselectivity (94/6 er) but with a much lower conversion (entry 10). In addition, other nickel sources, such as Ni(cod)$_2$, could also produce **3aa** with a comparable outcome (78 % yield, 95/5 er, entry 11). Other metal catalysts, such as $CrCl_2$, were completely ineffective in the formation of **3aa**, and undesired product **5aa** through allenylation of the aldehyde group was observed in a low yield (entry 12).[19a] To investigate the reactivity of leaving groups, we also screened different electrophiles in the reactions. Propargylic bromide **1a′** resulted in less efficiency and a large amount of byproduct **4aa**, most likely due to the higher reactivity to form the propargylic radical species; however, the enantiose-

Table 1: Optimization of reaction conditions.[a]

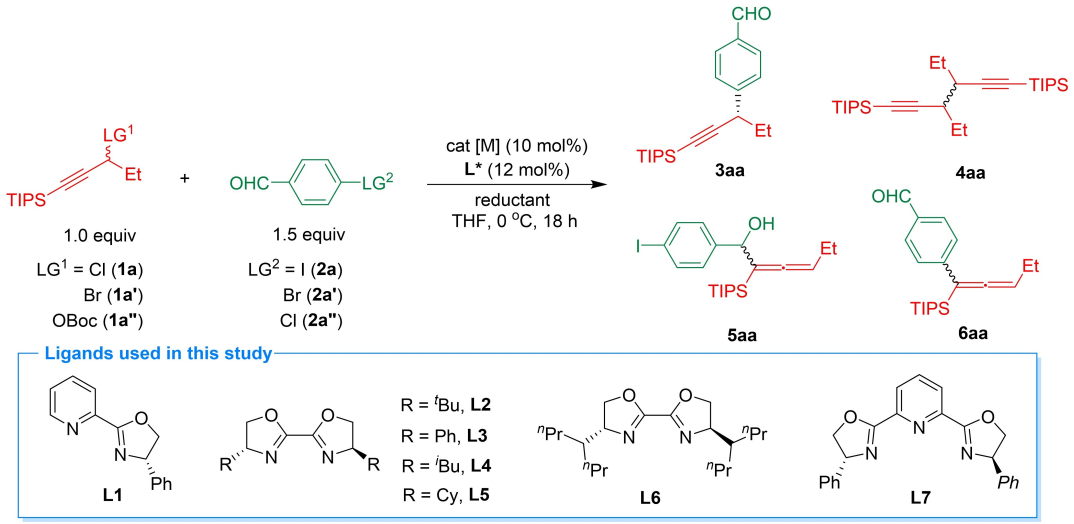

entry	LG^1	LG^2	cat [M] (mol%)	L* (mol%)	Reductant (equiv)	T °C	er of **3aa** (%)[b]	Yield of **3aa** (%)[c]
1	Cl (**1a**)	I (**2a**)	$NiBr_2$·dme (10)	(*S*)-**L1** (12)	Mn (3.0)	0	–	0
2	Cl (**1a**)	I (**2a**)	$NiBr_2$·dme (10)	(*R*, *R*)-**L2** (12)	Mn (3.0)	0	–	<5%
3	Cl (**1a**)	I (**2a**)	$NiBr_2$·dme (10)	(*R*, *R*)-**L3** (12)	Mn (3.0)	0	89/11	76
4	Cl (**1a**)	I (**2a**)	$NiBr_2$·dme (10)	(*R*, *R*)-**L4** (12)	Mn (3.0)	0	91/9	93
5	Cl (**1a**)	I (**2a**)	$NiBr_2$·dme (10)	(*R*, *R*)-**L5** (12)	Mn (3.0)	0	92/8	79
6	Cl (**1a**)	I (**2a**)	$NiBr_2$·dme (10)	(*R*, *R*)-**L6** (12)	Mn (3.0)	0	95.5/4.5	93
7	Cl (**1a**)	I (**2a**)	$NiBr_2$·dme (10)	(*R*, *R*)-**L7** (12)	Mn (3.0)	0	–	0
8	Cl (**1a**)	I (**2a**)	$NiBr_2$·dme (10)	(*R*, *R*)-**L6** (12)	Mn (3.0)	r.t.	93.5/6.5	95
9	Cl (**1a**)	I (**2a**)	$NiBr_2$·dme (10)	(*R*, *R*)-**L6** (12)	Mn (2.0)	0	95/5	89
10	Cl (**1a**)	I (**2a**)	$NiBr_2$·dme (10)	(*R*, *R*)-**L6** (12)	Zn (3.0)	0	94/6	54
11	Cl (**1a**)	I (**2a**)	$Ni(cod)_2$ (10)	(*R*, *R*)-**L6** (12)	Mn (3.0)	0	95/5	78
12	Cl (**1a**)	I (**2a**)	$CrCl_2$ (10)	(*R*, *R*)-**L6** (12)	Mn (3.0)	0	–	0
13	Br (**1a'**)	I (**2a**)	$NiBr_2$·dme (10)	(*R*, *R*)-**L6** (12)	Mn (3.0)	0	95.5/4.5	21
14	OBoc (**1a''**)	I (**2a**)	$NiBr_2$·dme (10)	(*R*, *R*)-**L6** (12)	Mn (3.0)	0	–	trace
15	Cl (**1a**)	Br (**2a'**)	$NiBr_2$·dme (10)	(*R*, *R*)-**L6** (12)	Mn (3.0)	0	–	trace
16	Cl (**1a**)	Cl (**2a''**)	$NiBr_2$·dme (10)	(*R*, *R*)-**L6** (12)	Mn (3.0)	0	–	0
17[d]	**Cl (1a)**	**I (2a)**	**$NiBr_2$·dme (10)**	**(*R*, *R*)-L6 (12)**	**Mn (3.0)**	**0**	**96/4**	**98 (95)**[e]
18[d]	Cl (**1a**)	I (**2a**)	$NiBr_2$·dme (5)	(*R*, *R*)-**L6** (6)	Mn (3.0)	0	96/4	85
19	Cl (**1a**)	I (**2a**)	$NiBr_2$·dme (10)	(*R*, *R*)-**L6** (6)	-	0	–	0
20	Cl (**1a**)	I (**2a**)	–	(*R*, *R*)-**L6** (12)	Mn (3.0)	0	–	0

[a] Reaction conditions: cat [M] (5–10 mol%), L* (6–12 mol%), **1a** (0.10 mmol), **2a** (0.15 mmol), reductant (0.30 mmol) in 1 mL of THF at 0 °C for 18 hours under argon. [b] Enantiomeric ratio (er) was determined by chiral HPLC analysis. [c] Yield was determined by GC analysis. [d] The solution of $NiBr_2$·dme and (*R, R*)-**L6** in THF was sonicated for 1 min before addition to reactants. [e] Isolated yield.

lectivity of the product could be maintained (entry 13). When the related propargylic *tert*-butyl carbonate **1a''** was employed, the reaction showed extremely low reactivity (entry 14). Furthermore, replacing 4-bromobenzaldehyde (**2a'**) or 4-chlorobenzaldehyde (**2a''**) with **2a** in the system made the reaction very sluggish (entries 15–16). Treatment of a solution of $NiBr_2$·dme and (*R, R*)-**L6** in THF, which was sonicated for 1 min before it was added to reactants, could further improve the outcome of the reaction, forming product **3aa** in 98% yield and 96/4 er (entry 17). Under the reaction conditions, lowering the loading of nickel catalyst to 5 mol% could also maintain good reactivity (85% yield, 96/4 er, entry 18). Finally, two control experiments revealed that the cross-coupling and dimerization of propargylic chloride **1a** did not proceed without reductant or nickel catalyst (entries 19–20). Notably, the allenylative arylation product **6aa** was not observed in any of the entries.

With the optimal conditions for the asymmetric propargyl-aryl coupling in hand, we next investigated the scope with respect to the different propargylic chlorides (Table 2). The reaction of iodoarene **2a** with diverse propargylic chlorides bearing a phenethyl (**1b**), an isopropyl (**1c**), a cyclobutyl (**1d**), a cyclohexyl (**1e**), a tetrahydro-2*H*-pyran-4-yl (**1f**), and a benzyl (**1g**) were compatible with this reaction. Note that excellent outcomes were obtained from propargylic chlorides containing heterocyclic skeletons, such as furan (**1h**) and thiophene (**1i**). The installation of the OBn group in propargylic chloride **1j** was tolerated to form product **3ja** in 82% yield and 91/9 er, but the coupling of substrate **1k** with an ester motif led to product **3ka** with a dramatically decreased yield (35%, 92/8 er), possibly due to

Table 2: Substrate scope of propargyl chlorides.[a]

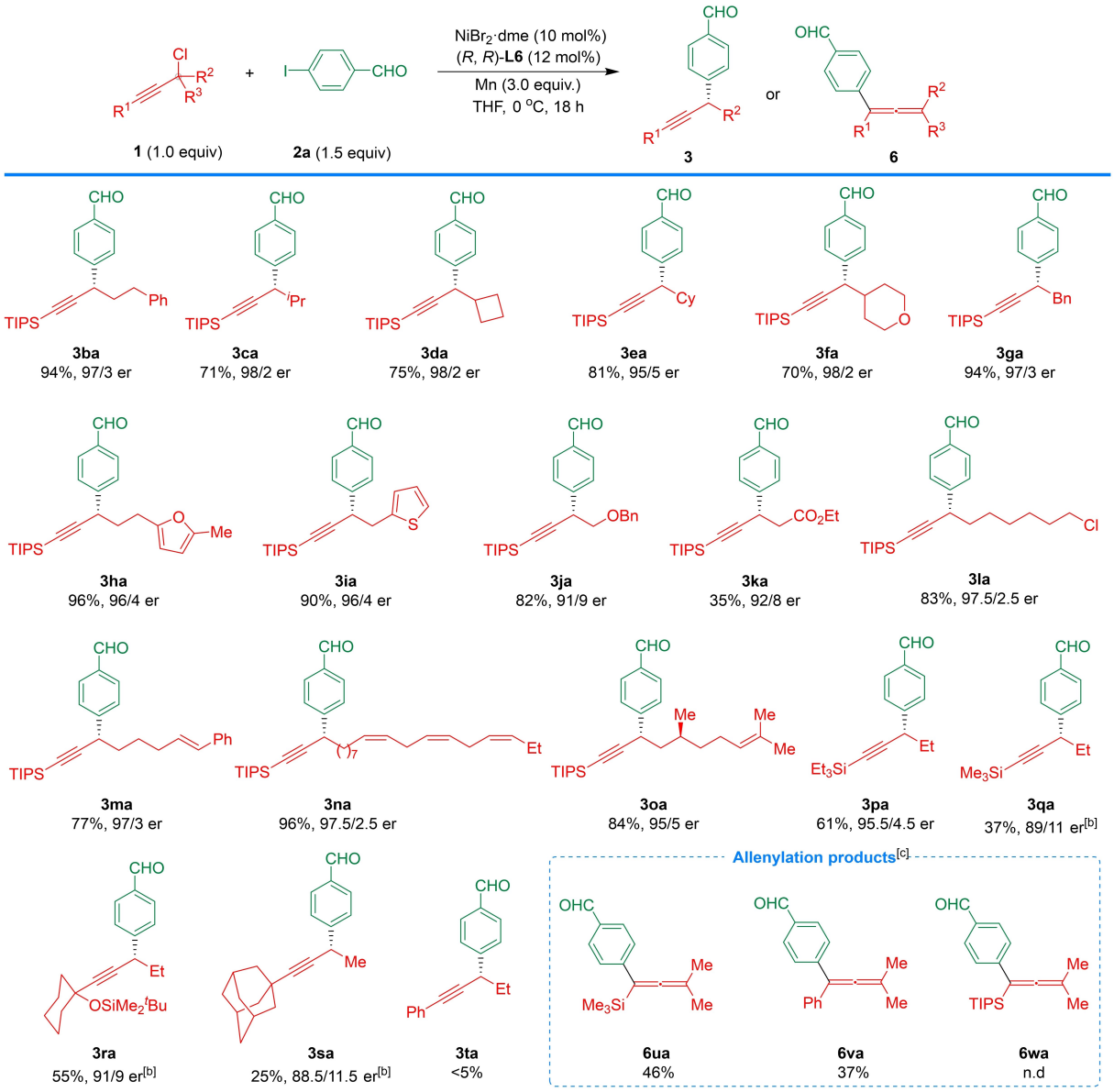

[a] Reaction conditions: $NiBr_2$·dme (10 mol%), (*R, R*)-**L6** (12 mol%), **1** (0.10 mmol), **2a** (0.15 mmol), Mn (0.30 mmol) in 1.0 mL of THF at 0 °C for 18 hours under argon; [b] For 48 h; [c] Reaction conditions: $Ni(cod)_2$ (10 mol%), 4,4′-diMeO-bpy (12 mol%), CoPc (5 mol%), **1** (0.10 mmol), **2a** (0.15 mmol), Mn (0.30 mmol) in 1.0 mL of THF at 0 °C for 18 hours under argon.

the β-H elimination of the generated propargylic radical. The observation that the coupling of compound **2l** bearing two different C–Cl bonds selectively provided product **3la** in 83% and 97.5/2.5 er shows that C–C bond formation occurs preferentially at the propargylic position. Substrate **1m** bearing a double bond did not interfere with the coupling event. Compound **1n**, which is derived from α-linolenic acid with three *cis* double bonds, was compatible with excellent configuration retention. The derivative of citronellal (**1o**) was also shown to be compatible with our system, affording product **3oa** with an excellent diastereomeric excess (de). In addition, propargylic chlorides bearing other silyl substituents at terminal positions, such as Et_3Si (**1p**) and Me_3Si (**1q**), also facilitated the formation of desired products **3pa** and **3qa** with acceptable ers (89/11–95.5/4.5); the enantiocontrol decreased gradually, with a decrease in steric hindrance of silyl motifs. In addition to silyl-substituted substrates, propargylic chlorides with a bulky silyl ether (**1r**) or adamantan-1-yl (**1s**) group could also participate in the reactions to form products **3ra** and **3sa** with modest outcomes. However, phenyl-substituted substrate **1t** was problematic under the current reaction conditions. With the success of secondary propargyl chlorides in the cross-coupling, we further investigated the related tertiary electrophiles in these catalytic systems. However, the reactions between propargyl chlorides **1u–v** and iodoar-

ene **2a** were more prone to form tetrasubstituted allenes **6ua** and **6va** under the modified reaction conditions, and bulky TIPS-substituted substrate **1w** failed to generate any coupling products.

We further examined the scope with respect to aryl and heteroaryl iodides (Table 3). Iodoarenes bearing diverse mono-substituted electron-withdrawing groups, such as acyl (**2b–d**), ester (**2e**), and cyano (**2f**), furnished corresponding products **3ab–af** in excellent ers. Multisubstituted aryl iodides **2g–i** with two electron-withdrawing groups could also generate desired adducts **3ag–ai** in excellent yields and enantioselectivities. However, for substrates with a strong electron-donating group, such as OMe (**2k**), at the *para* position, reduced enantioselectivity was observed in the

Table 3: Substrate scope of aryl and heteroaryl iodides.[a]

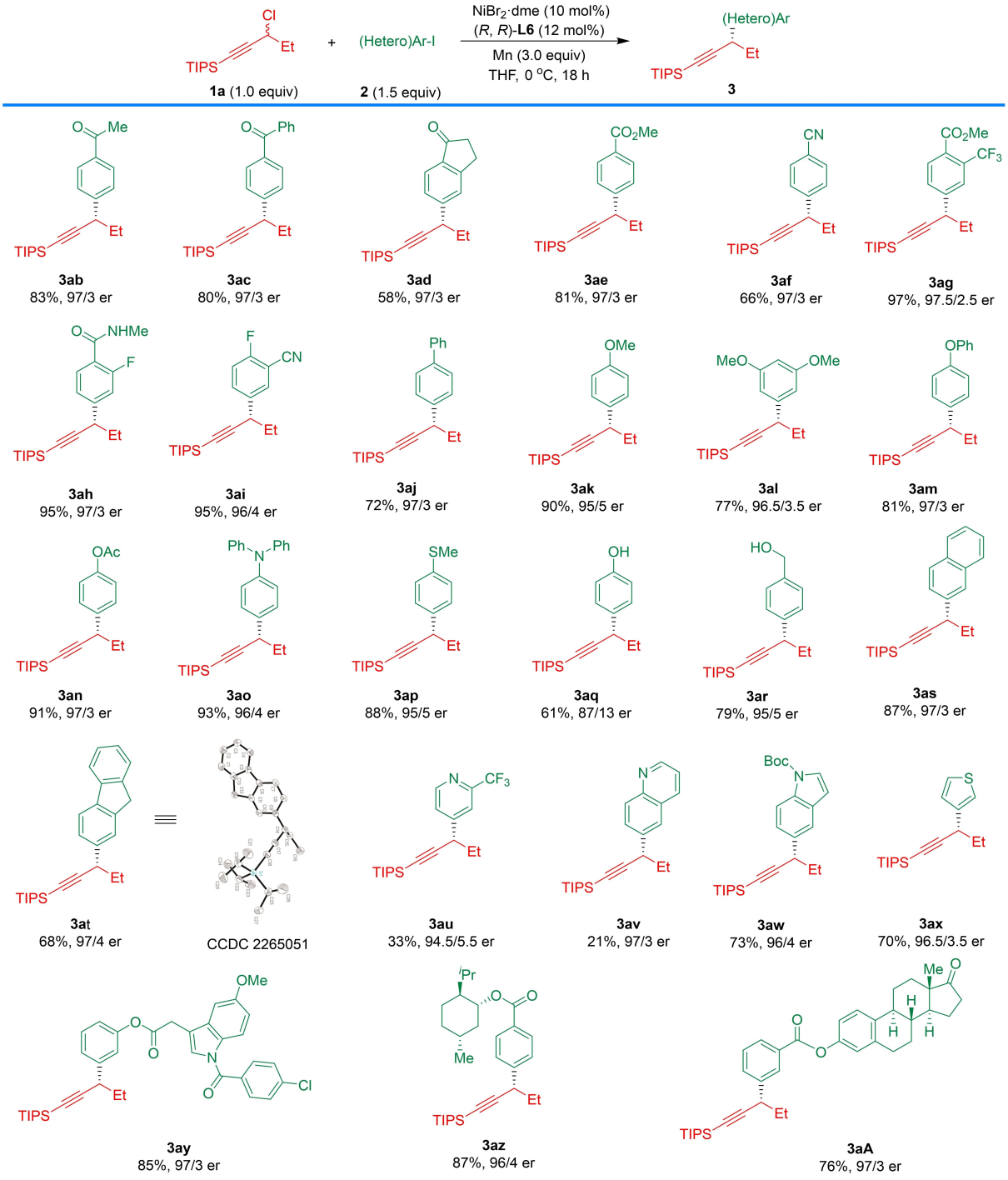

[a] Reaction conditions: $NiBr_2$·dme (10 mol%), (*R, R*)-**L6** (12 mol%), **1a** (0.10 mmol), **2** (0.15 mmol), Mn (0.30 mmol) in 1.0 mL of THF at 0 °C for 18 hours under argon.

formation of product **3ak** (95/5 er). However, iodoarenes bearing the two *meta* OMe groups and other *para*-substituted electron-donating groups, including phenoxy (**2m**), acetoxy (**2n**), tertiary amino (**2o**), and thioether (**2p**), could be well accommodated. In addition, the hydroxyl groups (**2q–r**) in the substrates can also survive mild reaction conditions, but the installation of the phenol motif resulted in modest enantioselectivity (**3aq**, 87/13 er). Polycyclic arenes **2s–t** were tolerated under the reaction conditions, and the *S* absolute configuration of product **3at** was confirmed by X-ray diffraction.[22] Heteroaryl iodides were readily accommodated in the transformation as follows: pyridine **2u** and quinoline **2v** were functionalized with good enantioselectivities (94.5/5.5–97/3 er), albeit with much lower reactivity, but indole **2w** and thiophene **2x** were readily converted into the corresponding products **3aw–ax** with good results. A major benefit of this mild and highly enantioselective reaction is the tolerance of a range of functional units commonly present in biologically active molecules. For example, indomethacin-derived molecule **2y** readily produced desired product **3ay** in 85% yield with 97/3 er. *L*–Menthol analog **2z** with three chiral centers could be subjected to this method to generate product **3az** in 87% yield with excellent de. In addition, a complex molecule **2 A** derived from estrone showed good outcome in the reaction.

To demonstrate the synthetic utility of this methodology, a series of experiments were further performed (Figure 2). Given that metallaphotoredox catalysis has emerged in recent years as a useful cross-coupling strategy with transition metal catalysis, we envisioned that propargyl-aryl

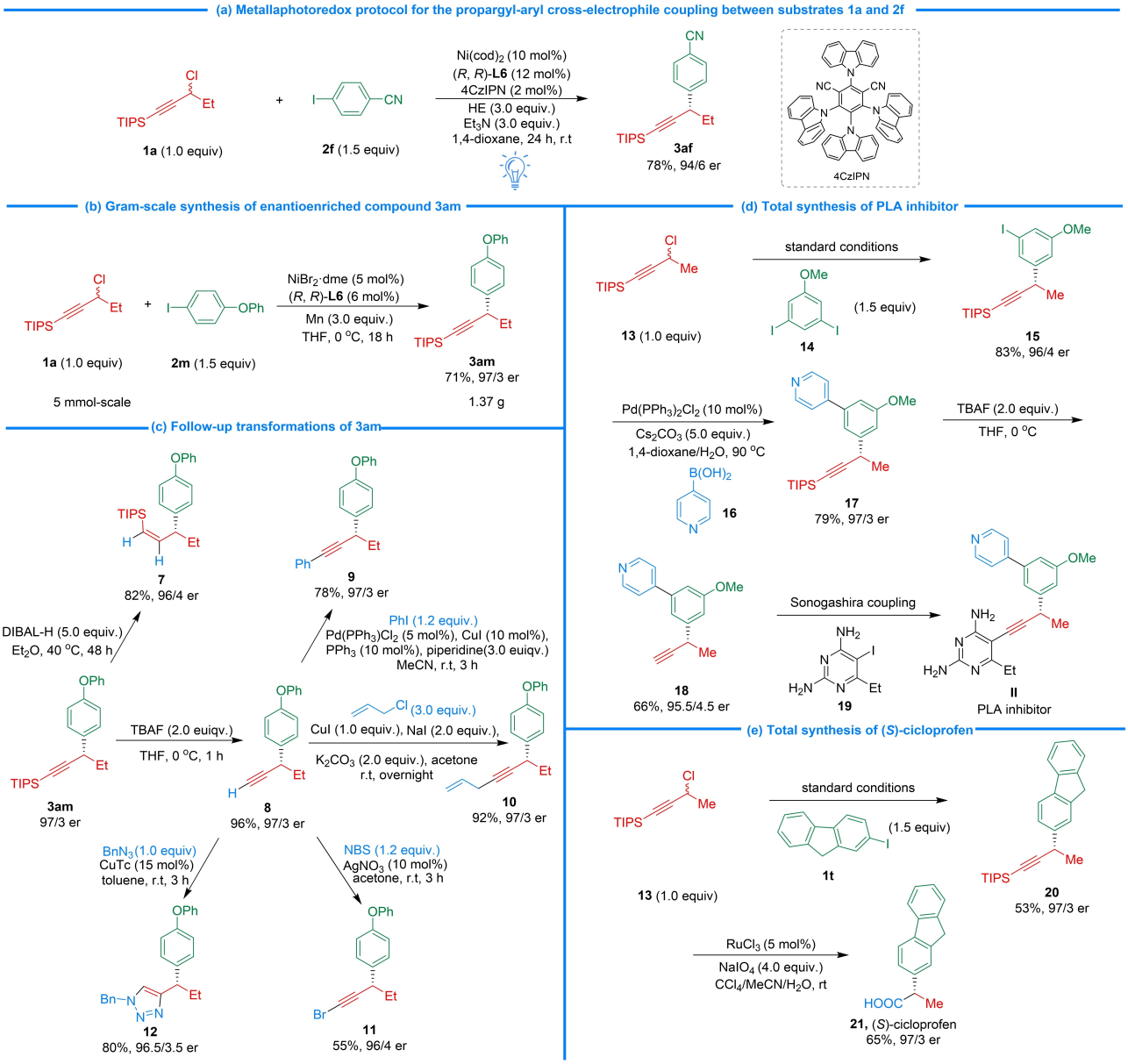

Figure 2. Further investigation of reaction conditions and synthetic applications.

cross-electrophile coupling might be conducted by a dual nickel/photoredox catalytic protocol without the use of a metal reductant.[23] Preliminary studies into the reaction were performed with propargylic chloride **1a**, iodoarene **2f**, 4CzIPN (2 mol %), $Ni(cod)_2$ (10 mol %), (*R, R*)-**L6** (12 mol %), Hantzsch ester and Et_3N, with exposure to a 40 W blue LED light source (456 nm) in 1,4-dioxane, delivering the desired product **3af** in 78 % yield with 94/6 er (Figure 2a). Using propargylic chloride **1a** and iodoarene **2m** as substrates, a gram-scale synthesis was smoothly carried out in 5.0 mmol with a reduced catalyst loading (5.0 mol % of $NiBr_2$·dme and 6.0 mol % of **L6**), and product **3am** was furnished in 71 % yield without loss of any enantioselectivity (Figure 2b). As noted at the outset, alkynyl products are extremely versatile intermediates in organic synthesis, as they can be converted into other important families of compounds. Several illustrative examples are provided in Figure 2c. The semihydrogenation of **3am** with DIBAL–H furnished *cis*-alkene **7** in 82 % yield and 96/4 er. More importantly, further derivatizations of **3am** can be achieved with synthetically useful terminal alkyne **8**, which was obtained in 96 % yield by the TBAF-mediated removal of the TIPS group. For instance, palladium-catalyzed Sonogashira coupling of **8** with PhI can generate internal alkyne product **9** in 78 % yield. A 1,4-enyne **10** (92 %, 97/3 er) can be synthesized smoothly from compound **8** and allyl chloride by copper catalysis. Bromination of compound **8** by silver catalyst formed product **11** without erosion of the enantiopurity. Alkyne **8** could also participate in a copper-catalyzed click reaction with BnN_3, affording triazole product **12** in 80 % yield with 96.5/3.5 er. The utility of our strategy can be further exemplified by its use in a key step in the asymmetric synthesis of biologically active molecules. To start the first synthesis, molecule **II** was prepared as a propargyl-linked antifolate, which is potent at both the enzymatic and cellular levels against wild-type and mutant F98Y dihydrofolate reductase (Figure 2d). The reaction of propargylic chloride **13** with 1,3-diiodo-5-methoxybenzene (**14**) under the optimized conditions formed key intermediate **15** in 83 % yield and 96/4 er. The subsequent Suzuki–Miyaura coupling of compound **15** with pyridin-4-ylboronic acid (**16**) using a catalytic amount of $Pd(PPh_3)_2Cl_2$ led to product **17** in 79 % yield and 97/3 er. Further deprotection of the silyl group in **17** produced terminal alkyne **18**, which could be converted into the target by Pd-catalyzed Sonogashira coupling with heteroaryl iodide **19**. Based on alkyne conversion, the formed triple bond could be used as a precursor of carboxyl acid in drug synthesis (Figure 2e). For example, the propargyl-aryl cross-electrophile coupling of substrate **13** with iodoarene **1t** under the developed conditions furnished product **20** in 53 % yield with 97/3 er, and further oxidative cleavage of the C–C triple bond yielded (*S*)-cicloprofen **21** as a nonsteroidal anti-inflammatory drug in 65 % yield with 97/3 er. These examples clearly demonstrate that the new strategy for propargylic arylation is well suited to the rapid and modular construction of complex molecules.

To provide insight into the reaction mechanism, a series of experiments were then conducted (Figure 3). We first tested optically active propargylic chloride *S*-**13** in the cross-electrophile coupling with iodoarene **2l** using dtbbpy as a ligand, affording racemic product **23** in 73 % yield (Figure 3a). This result ruled out an S_N2 pathway involving the addition of a catalytically generated aryl-Ni species to the propargylic chloides.[11] When stoichiometric amounts of TEMPO (2,2-6,6-tetramethyl piperidine-*N*-oxyl) were added under standard conditions, the reaction was immensely inhibited (Figure 3b). Furthermore, the addition of two equivalents of allylic sulfone **23** to the system furnished **3aa** in a diminished yield (71 %), and allylic adduct **24** was isolated in 14 % yield. This result supports the formation of propargylic radicals in this transformation. When 3.0 equiv. of iodoarene **2e** was reacted with 1.0 equiv. of $Ni(cod)_2$ and ligand (*R, R*)-**L6**, nickel complex **25** was obtained and confirmed by X-ray analysis (Figure 3c).[22] There are two ligands with one nickel species in complex **25**, and its geometry indicates the six-coordinate around nickel atoms is quite close to octahedron. We further attempted to synthesize the monomeric species from $NiBr_2$·dme and ligand **L6**. To our surprise, dimeric species **26** and trimeric species **27** were isolated and confirmed by X-ray analysis (Figure 3d). We speculate that dynamic equilibrium occurs among the monomeric, dimeric and trimeric species, in which the aggregated forms are thermodynamically more stable. Furthermore, control reactions revealed that complex **25** showed low reactivity, and product **3aa** was obtained in comparable yields and er values using either dimeric or trimeric species (Figure 3e). Different from the previous reported mechanism of the free radical generation,[23] control experiments demonstrated the crucial role of Ni(I) in the generation of propargyl radicals (Figure 3f). It is worth noting that manganese, nickel(II), and nickel(0), when used separately, cannot generate free radicals. However, the combination of nickel(II) catalyst with reducing agent manganese significantly enhances reaction activity, indicating the occurrence of single-electron transfer between Ni(I) species and **2a**. Nonlinear effect (NLE) study on the enantiomeric composition of chiral ligand (*R, R*)-**L6** and the product **3aa** was performed under the optimized reaction conditions (Figure 3g).[24] Significant linear correlation were observed, supporting that the monomer nickel complex with the bidentate chiral ligand [Ni/**L6** = 1 : 1] is the most likely active species in asymmetric reactions. During the investigation of the substrate scope of aryl iodides, we observed that substrate **2k** bearing a strongly electron-donating OMe group at the *para* position was effectively converted into corresponding product **3ak** but with a slightly diminished er value (95/5 er).

Interestingly, a simple plot of the correlation between a log of enantioselectivity (er) and the σ-Hammett parameters of aryl substituents shows an almost linear correlation (R^2 = 0.9513; Figure 3h). As a result, the electronic variations in the aryl electrophile significantly affect the enantioselectivity of propargyl-aryl cross-electrophile coupling. The positive slope (0.2508) suggests enantioselectivity increases as the substituents shifted from electron-donating group to electron-withdrawing group.

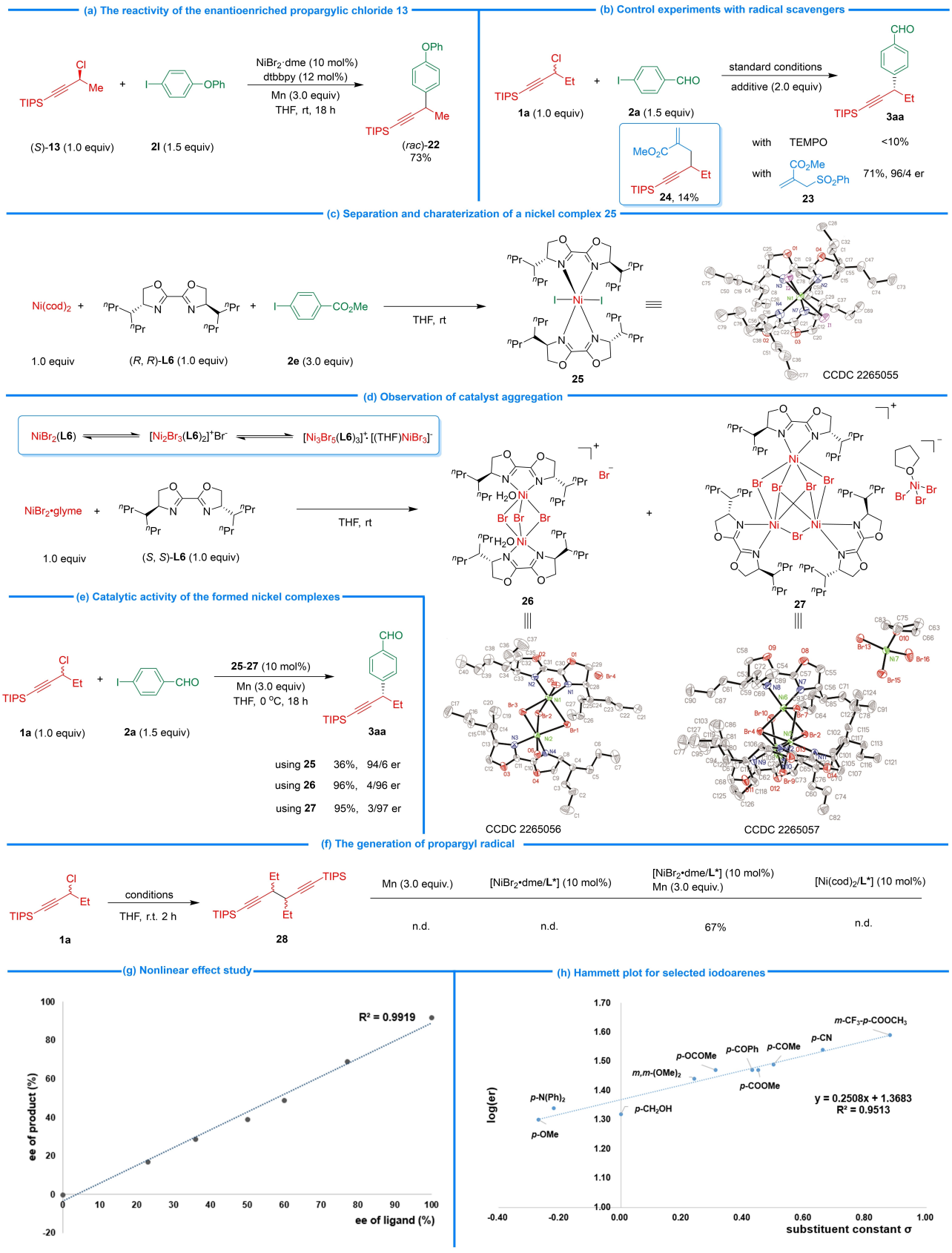

Figure 3. Mechanistic studies.

Based on the above experimental results and literature reports,[25] density functional theory (DFT) calculations were then performed to elucidate the detailed mechanism of the nickel-catalyzed asymmetric propargyl-aryl cross-electrophile coupling and the role of the chiral ligand (*R*, *R*)-**L6** on enantioselectivity (Figure 4).[26] It is shown in Table 1 that

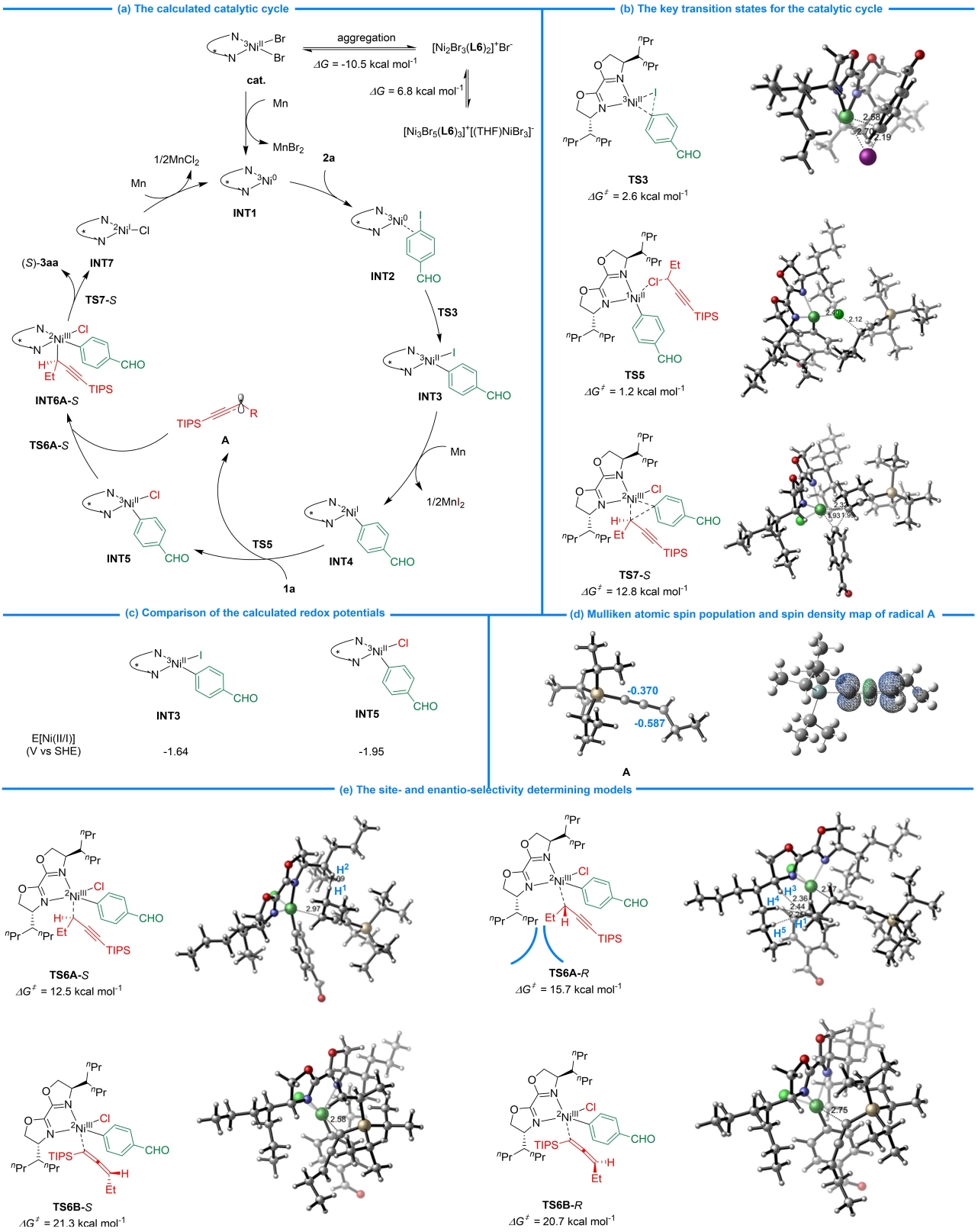

Figure 4. DFT investigation.

nickel(0) exhibits comparable enantioselectivity to nickel(II) under the standard condition, suggesting that Ni(0) may be the active catalyst entering into the catalytic cycle (entry 11, Table 1). Initially, the Ni(II) pre-catalyst is reduced by Mn to form the open-shell Ni(0) species **INT1** with tetrahedral geometry (Figure 4a, see Supporting Information for the detailed free energy profile of the proposed mechanism). The generated **INT1** coordinates with substrate **2a** and then undergoes oxidative addition with the C–I bond through transition state **TS3** with an activation energy of 2.6 kcal mol^{-1} to furnish intermediate **INT3** (Figure 4b). Upon reduction by excess Mn, aryl-Ni(I) species **INT4** is formed, which triggers a halogen atom transfer from **1a** through transition state **TS5** to generate radical **A**, simultaneously leading to the formation of Ni(II) species **INT5**. The calculated redox potentials indicated that **INT5** has lower oxidizability compared to **INT3** and is difficult to be reduced by reducing agent Mn, which effectively excludes the reaction mechanism involving Ni(0)-Ni(II)-Ni(I)-Ni(II)-Ni-(0) pathway (Figure 4c). The regioselectivity and enantioselectivity in the reaction mechanism are closely related to the electronic nature of the free radical **A** and the steric hindrance of the transition states. Structural analysis shows that radical **A** adopts a linear geometry, with the γ-carbon atom attached to the ethyl (Et) group (with a Mulliken charge of −0.587) being more negative than the α-carbon atom next to the triisopropylsilyl (TIPS) group (with a Mulliken charge of −0.370) (Figure 4d). Additionally, the spin density analysis of radical **A** reveals that the γ-carbon atom exhibits more significant radical character than the α-carbon atom. These calculational results clarify the more nucleophilic nature of the γ-carbon atom in radical **A**; making it more prone to being intercepted by intermediate **INT5** to form propargylic-Ni(III) species **INT6A**, rather than producing allenylation species **INT6B**. The intermolecular radical addition occurs through transition states **TS6A**-*S* and **TS6A**-*R* with energy barriers of 12.5 and 15.7 kcal mol^{-1}, respectively. These energy barriers are much lower compared to the alternative pathways through transition states **TS6B**-*S* and **TS6B**-*R* (12.5 and 15.7 kcal mol^{-1} vs. 21.3 and 20.7 kcal mol^{-1}) (Figure 4e). The significant difference in activation energy barriers between the two radical addition pathways is mainly due to the lower repulsive interactions between the ethyl group and chiral ligand in **TS6 A**-*S* and **TS6A**-*R* compared to those between TIPS groups and chiral ligand in less favorable **TS6B**-*S* and **TS6B**-*R*. This result highlights the significant role of bulky TIPS substituents in controlling the enantioselectivity of the propargylic center. Reducing the steric hindrance of TIPS or increasing the steric hindrance of the propargylic position promotes the generation of allene products, and the isolation of **6ua** and **6va** provides experimental support for this conclusion. The origin of enantioselectivity can be further elaborated by the enantioselectivity-determining model. The pathway determining the observed *S*-configuration via **TS6A**-*S* is 3.2 kcal mol^{-1} more favorable than that used to determine the *R*-configuration pathway (12.5 vs. 15.7 kcal mol^{-1}). Based on computational analysis, the disfavored transition state **TS6A**-*R* suffers from greater steric repulsion, as evidenced by the shorter distances of H^1-H^3 (2.36 Å), H^1-H^4 (2.44 Å), and H^1-H^5 (2.25 Å); thus, the energy barrier of **TS6A**-*R* for generating the *R* isomer is increased, which is in line with the experimentally observed enantioselectivity. Similar findings have been reported that radical addition to tetrahedral Ni(II) center, rather than the reductive elimination, is the enantio-determining step.[15h,27] The following reductive elimination of intermediate **INT6A**-*S* occurs through transition state **TS7**-*S* with an activation energy of 12.8 kcal mol^{-1} to yield desired product (*S*)-**3aa** while regenerating active catalyst **INT1** to complete the catalytic cycle after reduction by Mn.

Conclusion

In summary, we established an asymmetric nickel-catalyzed propargylic arylation via cross-electrophile coupling. The reaction utilized bench-stable propargylic chlorides and aryl iodides as coupling partners and manganese as a stoichiometric reductant, avoiding the necessity of prepared organometallic nucleophiles. The mild reaction conditions featured a wide range of benzylic alkynes bearing diverse functionalities in high yields with terrific ee values. A positive linear correlation between substituent constants σ and enantiopurities of products helped predict suitable substrates in this transformation. Detailed mechanistic investigations revealed that the origins of the reaction site and enantioselectivity are derived from steric effects.

Acknowledgements

Financial support from National Key R&D Program of China (2022YFA1503200), National Natural Science Foundation of China (Grants 22025104, 22171134, 21972064 and 21901111), and the Fundamental Research Funds for the Central Universities (Grant 020514380254) for their financial support. The project is also supported by Open Research Fund of School of Chemistry and Chemical Engineering, Henan Normal University. We are also grateful to the High-Performance Computing Center of Nanjing University for performing the numerical calculations in this paper on its blade cluster system.

Conflict of Interest

The authors declare no conflict of interest.

Data Availability Statement

The data that support the findings of this study are available in the supplementary material of this article.

Keywords: Cross-Coupling · Density Functional Theory · Enantioselectivity · Nickel Catalysis · Stereoconvergent

[1] a) B. M. Trost, & C. J. Li, *Modern Alkyne Chemistry: Catalytic and Atom-Economic Transformations*; Wiley-VCH, Weinheim, **2014**; b) F. Diederich, P. J. Stang, R. R. Tykwinski, *Acetylene Chemistry Chemistry, Biology and Material Science*; Wiley-VCH: Weinheim, **2005**; c) D. Huang, Y. Liu, A.-J. Qin, B.-Z. Tang, *Polym. Chem.* **2018**, *9*, 2853–2867.

[2] a) I. T. Trotuş, T. Zimmermann, F. Schüth, *Chem. Rev.* **2014**, *114*, 1761–1782; b) V. K. Tiwari, B. B. Mishra, K. B. Mishra, N. Mishra, A. S. Singh, X. Chen, *Chem. Rev.* **2016**, *116*, 3086–3240.

[3] a) L. Fu, S. Zhou, X. Wan, P. Chen, G. Liu, *J. Am. Chem. Soc.* **2018**, *140*, 10965–10969; b) H. Xia, Z.-L. Li, Q.-S. Gu, X.-Y. Dong, J.-H. Fang, X.-Y. Du, L.-L. Wang, X.-Y. Liu, *Angew. Chem. Int. Ed.* **2020**, *59*, 16926–16932; c) X. Jiang, B. Han, Y. Xue, M. Duan, Z. Gui, Y. Wang, S. Zhu, *Nat. Commun.* **2021**, *12*, 3792; d) A. E. Wendlandt, P. Vangal, E. N. Jacobsen, *Nature* **2018**, *556*, 447–451.

[4] Y. Nishibayashi, I. Wakiji, M. Hidai, *J. Am. Chem. Soc.* **2000**, *122*, 11019–11020.

[5] a) G. Hattori, K. Sakata, H. Matsuzawa, Y. Tanabe, Y. Miyake, Y. Nishibayashi, *J. Am. Chem. Soc.* **2010**, *132*, 10592–10608; b) K. Nakajima, M. Shibata, Y. Nishibayashi, *J. Am. Chem. Soc.* **2015**, *137*, 2472–2475; c) R.-Z. Li, H. Tang, K. R. Yang, L.-Q. Wan, X. Zhang, J. Liu, Z. Fu, D. Niu, *Angew. Chem. Int. Ed.* **2017**, *56*, 7213–7217; d) R.-Z. Li, D.-Q. Liu, D. Niu, *Nat. Catal.* **2020**, *3*, 672–680.

[6] a) H. Huo, B. J. Gorsline, G. C. Fu, *Science* **2020**, *367*, 559–564; b) S. W. Smith, G. C. Fu, *Angew. Chem. Int. Ed.* **2008**, *47*, 9334–9336; c) Y. Miyake, S. Uemura, Y. Nishibayashi, *ChemCatChem* **2009**, *1*, 342–356; d) N. Ljungdahl, N. Kann, *Angew. Chem. Int. Ed.* **2009**, *48*, 642–644; e) F.-D. Lu, D. Liu, L. Zhu, L.-Q. Lu, Q. Yang, Q.-Q. Zhou, Y. Wei, Y. Lan, W.-J. Xiao, *J. Am. Chem. Soc.* **2019**, *141*, 6167–6172.

[7] a) X. Chang, J. Zhang, L. Peng, C. Guo, *Nat. Commun.* **2021**, *12*, 299; b) L. Peng, Z. He, X. Xu, C. Guo, *Angew. Chem. Int. Ed.* **2020**, *59*, 14270–14274; c) X. Xu, L. Peng, X. Chang, C. Guo, *J. Am. Chem. Soc.* **2021**, *143*, 21048–21055; d) Q. Hu, Z. He, L. Peng, C. Guo, *Nat. Synth.* **2022**, *1*, 322–331; e) Z. He, L. Peng, C. Guo, *Nat. Synth.* **2022**, *1*, 393–400.

[8] a) S. W. Smith, G. C. Fu, *J. Am. Chem. Soc.* **2008**, *130*, 12645–12647; b) N. D. Schley, G. C. Fu, *J. Am. Chem. Soc.* **2014**, *136*, 16588–16593.

[9] A. J. Oelke, J. Sun, G. C. Fu, *J. Am. Chem. Soc.* **2012**, *134*, 2966–2969.

[10] S. Jiang, X.-Y. Dong, Q.-S. Gu, L. Ye, Z.-L. Li, X.-Y. Liu, *J. Am. Chem. Soc.* **2020**, *142*, 19652–19659.

[11] M. Guisán-Ceinos, V. Martín-Heras, M. Tortosa, *J. Am. Chem. Soc.* **2017**, *139*, 8448–8451.

[12] a) X.-Y. Dong, Y.-F. Zhang, C.-L. Ma, Q.-S. Gu, F.-L. Wang, Z.-L. Li, S.-P. Jiang, X.-Y. Liu, *Nat. Chem.* **2019**, *11*, 1158–1166; b) F.-L. Wang, C.-J. Yang, J.-R. Liu, N.-Y. Yang, X.-Y. Dong, R.-Q. Jiang, X.-Y. Chang, Z.-L. Li, G.-X. Xu, D.-L. Yuan, Y.-S. Zhang, Q.-S. Gu, X. Hong, X.-Y. Liu, *Nat. Chem.* **2022**, *14*, 949–957.

[13] a) D. A. Everson, D. J. Weix, *J. Org. Chem.* **2014**, *79*, 4793–4798; b) C. E. I. Knappke, S. Grupe, D. Gartner, M. Corpet, C. Gosmini, A. Jacobi von Wangelin, *Chem. Eur. J.* **2014**, *20*, 6828–6842; c) T. Moragas, A. Correa, R. Martin, *Chem. Eur. J.* **2014**, *20*, 8242–8258; d) D. J. Weix, *Acc. Chem. Res.* **2015**, *48*, 1767–1775; e) J. Gu, X. Wang, W. Xue, H. Gong, *Org. Chem. Front.* **2015**, *2*, 1411–1421.

[14] a) M. F. Semmelhack, P. M. Helquist, L. D. Jones, *J. Am. Chem. Soc.* **1971**, *93*, 5908–5910; b) A. S. Kende, L. S. Liebeskind, D. M. Braitsch, *Tetrahedron Lett.* **1975**, *16*, 3375–3378; c) M. Zembayashi, K. Tamao, J. Yoshida, M. Kumada, *Tetrahedron Lett.* **1977**, *18*, 4089–4092.

[15] a) K. E. Poremba, S. E. Dibrell, S. E. Reisman, *ACS Catal.* **2020**, *10*, 8237–8246; b) B.-B. Wu, J. Xu, K.-J. Bian, Q. Gao, X.-S. Wang, *J. Am. Chem. Soc.* **2022**, *144*, 6543–6550; c) H. Wang, P. Zheng, X. Wu, Y. Li, T. Xu, *J. Am. Chem. Soc.* **2022**, *144*, 3989–3997; d) T. J. DeLano, S. E. Dibrell, C. R. Lacker, A. R. Pancoast, K. E. Poremba, L. Cleary, M. S. Sigman, S. E. Reisman, *Chem. Sci.* **2021**, *12*, 7758–7762; e) D. Sun, G. Ma, X. Zhao, C. Lei, H. Gong, *Chem. Sci.* **2021**, *12*, 5253–5258; f) H. Tu, F. Wang, L. Huo, Y. Li, S. Zhu, X. Zhao, H. Li, F.-L. Qing, L. Chu, *J. Am. Chem. Soc.* **2020**, *142*, 9604–9611; g) D. Anthony, Q. Lin, J. Baudet, T. Diao, *Angew. Chem. Int. Ed.* **2019**, *58*, 3198–3202; h) X. Wei, W. Shu, A. García-Domínguez, E. Merino, C. Nevado, *J. Am. Chem. Soc.* **2020**, *142*, 13515–13522; i) X. Wu, J. Qu, Y. Chen, *J. Am. Chem. Soc.* **2020**, *142*, 15654–15660; j) X. Jiang, W. Xiong, S. Deng, F.-D. Lu, Y. Jia, Q. Yang, L.-Y. Xue, X. Qi, J. A. Tunge, L.-Q. Lu, W.-J. Xiao, *Nat. Catal.* **2022**, *5*, 788–797; k) K. Wang, Z. Ding, Z. Zhou, W. Kong, *J. Am. Chem. Soc.* **2018**, *140*, 12364–12368.

[16] a) A. H. Cherney, N. T. Kadunce, S. E. Reisman, *J. Am. Chem. Soc.* **2013**, *135*, 7442–7445; b) A. H. Cherney, S. E. Reisman, *J. Am. Chem. Soc.* **2014**, *136*, 14365–14368; c) J. L. Hofstra, A. H. Cherney, C. M. Ordner, S. E. Reisman, *J. Am. Chem. Soc.* **2018**, *140*, 139–142; d) T. J. DeLano, S. E. Reisman, *ACS Catal.* **2019**, *9*, 6751–6754; e) K. E. Poremba, N. T. Kadunce, N. Suzuki, A. H. Cherney, S. E. Reisman, *J. Am. Chem. Soc.* **2017**, *139*, 5684–5687; f) N. Suzuki, J. L. Hofstra, K. E. Poremba, S. E. Reisman, *Org. Lett.* **2017**, *19*, 2150–2153.

[17] a) B. P. Woods, M. Orlandi, C.-Y. Huang, M. S. Sigman, A. G. Doyle, *J. Am. Chem. Soc.* **2017**, *139*, 5688–5691; b) S. H. Lau, M. A. Borden, T. J. Steiman, M. Parasram, L. S. Wang, A. G. Doyle, *J. Am. Chem. Soc.* **2021**, *143*, 15873–15881.

[18] Z. Zhu, L. Lin, J. Xiao, Z. Shi, *Angew. Chem. Int. Ed.* **2022**, *61*, e202113209.

[19] a) F.-H. Zhang, X. Guo, X. Zeng, Z. Wang, *Angew. Chem. Int. Ed.* **2022**, *61*, e202117114; b) Y. Jin, H. Wen, F. Yang, D. Ding, C. Wang, *ACS Catal.* **2021**, *11*, 13355–13362.

[20] a) M. Sakai, M. Ueda, N. Miyaura, *Angew. Chem. Int. Ed.* **1998**, *37*, 3279–73281; b) H-F. Duan, J.-H. Xie, W.-J. Shi, Q. Zhang, Q.-L. Zhou, *Org. Lett.* **2006**, *8*, 1479–1481; c) T. Nishimura, H. Kumamoto, M. Nagaosa, T. Hayashi, *Chem. Commun.* **2009**, *38*, 5713–5715; d) Y. Yamamoto, K. Kurihara, N. Miyaura, *Angew. Chem. Int. Ed.* **2009**, *48*, 4414–4416; e) S. Morikawa, K. Michigami, H. Amii, *Org. Lett.* **2010**, *12*, 2520–2523; f) C.-H. Xing, Y.-X. Liao, P. He, Q.-S. Hu, *Chem. Commun.* **2010**, *46*, 3010–3012; g) J. Karthikeyan, M. Jeganmohan, C.-H. Cheng, *Chem. Eur. J.* **2010**, *16*, 8989–8992; h) Z.-C. Wang, J. Gao, Y. Cai, X. Ye, S.-L. Shi, *CCS Chem.* **2021**, *4*, 1169–1179; i) Y. Cai, L.-X. Ruan, R. Abdul, S.-L. Shi, *Angew. Chem. Int. Ed.* **2021**, *60*, 5262–5267.

[21] a) K. E. Poremba, N. T. Kadunce, N. Suzuki, A. H. Cherney, S. E. Reisman, *J. Am. Chem. Soc.* **2018**, *140*, 7746–7746; b) B. P. Woods, M. Orlandi, C.-Y. Huang, M. S. Sigman, A. G. Doyle, *J. Am. Chem. Soc.* **2018**, *140*, 7744–7745; c) H. Guan, Q. Zhang, P. J. Walsh, J. Mao, *Angew. Chem. Int. Ed.* **2020**, *59*, 5172–5177.

[22] Single crystals of compounds **3at**, **25**, **26**, and **27**, were grown for X-ray analysis using the slow evaporation technique with a solvent mixture of DCM (or THF) and hexane at room temperature. Deposition numbers 2265051 (for **3at**), 2265055 (for **25**), 2265056 (for **26**), and 2265057 (for **27**) contain the supplementary crystallographic data for this paper. These data are provided free of charge by the joint Cambridge Crystallographic Data Centre and Fachinformationszentrum Karlsruhe Access Structures service.

[23] a) C. K. Prier, D. A. Rankic, D. W. C. MacMillan, *Chem. Rev.* **2013**, *113*, 5322–5363; b) M. N. Hopkinson, B. Sahoo, J. L. Li, F. Glorius, *Chem. Eur. J.* **2014**, *20*, 3874–3886; c) J. Twilton,

C. C. Le, P. Zhang, M. H. Shaw, R. W. Evans, D. W. C. MacMillan, *Nat. Chem. Rev.* **2017**, *1*, 0052; d) F.-D. Lu, J. Chen, X. Jiang, J.-R. Chen, L.-Q. Lu, W.-J. Xiao, *Chem. Soc. Rev.* **2021**, *50*, 12808–12827; e) A. Y. Chan, I. B. Perry, N. B. Bissonnette, B. F. Buksh, G. A. Edwards, L. I. Frye, O. L. Garry, M. N. Lavagnino, B. X. Li, Y. Liang, E. Mao, A. Millet, J. V. Oakley, N. L. Reed, H. A. Sakai, C. P. Seath, D. W. C. MacMillan, *Chem. Rev.* **2022**, *122*, 1485–1542.

[24] L. Ju, Q. Lin, N. J. LiBretto, C. L. Wagner, C. T. Hu, J. T. Miller, T. Diao, *J. Am. Chem. Soc.* **2021**, *143*, 14458–14463.

[25] a) D. Guillaneux, S.-H. Zhao, O. Samuel, D. Rainford, H. B. Kagan, *J. Am. Chem. Soc.* **1994**, *116*, 9430–9439; b) C. Girard, H. B. Kagan, *Angew. Chem. Int. Ed.* **1998**, *37*, 2922–2959; *Angew. Chem.* **1998**, *110*, 3088–3127.

[26] a) A. Duan, F. Xiao, Y. Lan, L. Niu, *Chem. Soc. Rev.* **2022**, *51*, 9986–10015; b) S. Biswas, D. J. Weix, *J. Am. Chem. Soc.* **2013**, *135*, 16192–16197; c) Q. Lin, E. H. Spielvogel, T. Diao, *Chem* **2023**, *9*, 1295–1308.

[27] All calculations were performed at the M06-D3/6–311+G-(d,p)-SDD/SMD(THF)-//B3LYP-D3/6-31G(d)-SDD/SMD-(THF) level of theory using Gaussian 09 software package (see Supporting Information for details). Furthermore, we found that using 2/3 of the entropy correction for ΔG values at 273 K provides results comparable with experimental data where available.

[28] a) M. Yuan, O. Gutierrez, *IREs Comput. Mol. Sci.* **2022**, *12*, e1573; b) H. Yin, G. C. Fu, *J. Am. Chem. Soc.* **2019**, *141*, 15433–15440; c) L. Guo, M. Yuan, Y. Zhang, F. Wang, S. Zhu, O. Gutierrez, L. Chu, *J. Am. Chem. Soc.* **2020**,*142*, 20390–20399.

Manuscript received: September 13, 2023
Accepted manuscript online: November 20, 2023
Version of record online: November 30, 2023